



**JOINT INSTITUTE FOR NUCLEAR RESEARCH**  
Veksler and Baldin laboratory of High Energy Physics

FINAL REPORT ON THE START PROGRAMME

*GEM residuals correction in carbon beam with various targets at  
4.5 GeV in Run 6 experimental data of the BM@N Experiment*

**Supervisor:**

Yury Stepanenko, Russia  
VBLHEP JINR

**Student:**

Rivu Adhikary, India  
NRNU MPhI

**Participation period:**

July 17 – September 03,  
Summer Session 2022

Dubna, 2022

## **Abstract.**

Located in the NICA-JINR complex, the BM@N (Baryonic Matter at Nuclotron) is a stationary target experiment designed to work with the Nuclotron extracted beams of different species. At nuclotron energies, we aim to study the equation-of-state (EoS) of strongly interacting matter at high temperatures and high net-baryon densities. In such heavy ion collisions, nucleons are excited to baryonic resonances which decay by the emission of lighter baryons and mesons. This paper discusses the processing of experimental data from Run 6 of the BM@N experiment. The run was carried out on a carbon (C) beam with various fixed targets, respectively, reactions C+C, C+Al, C+Cu, C+Pb at collision energies of 4.0 and 4.5 GeV.

In the current work, we analyze the dx-residual distributions of the reconstructed tracks in the six Gaseous Electron Multiplier detector (GEM) stations for 4.5 GeV collision energy and apply the method of the dx-residuals correction [1]. It is one of the crucial intermediary phases in the analysis of Run-6 data from the BM@N experiment. These corrections enable the estimation, comparison, and improvement of the track reconstruction procedure's accuracy for Monte-Carlo and physical events.

## **1 Introduction**

The gateway to explore the fundamental levels of matter is relativistic heavy ion collisions. These collisions are a unique opportunity to study nuclear matter under extremely high density and temperature conditions. The Nuclotron-based Ion Collider Facility (NICA) at Joint Institute for Nuclear Research (JINR) in Dubna, aims at investigating elementary reactions (pp, pA) and the properties of dense baryonic matter formed in course of such heavy-ion collisions using the BM@N experiment. The schematic view of the NICA-Nuclotron complex and that of the BM@N setup are presented in Figures 1 and 2 respectively.



Fig. 1 - NICA complex schematic layout

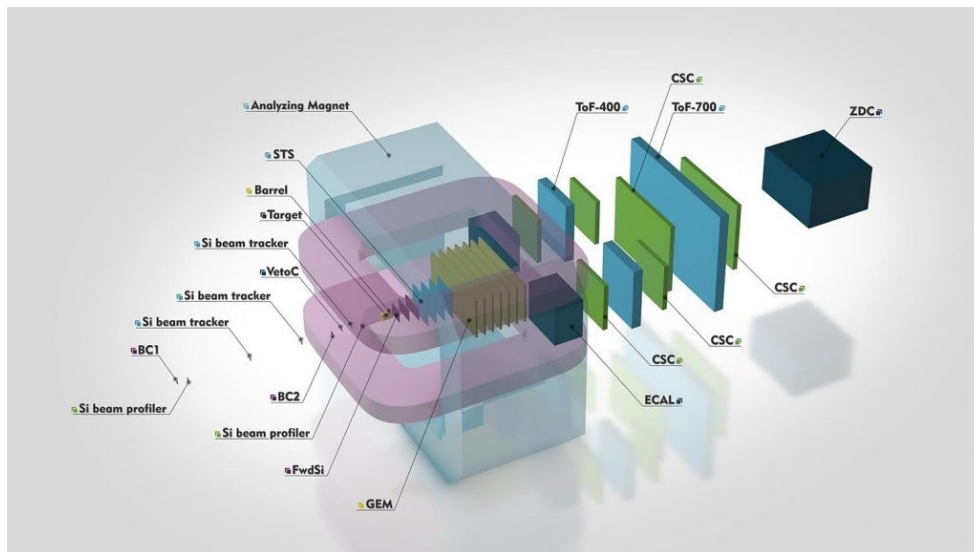


Fig. 2 - Schematic view of BM@N experimental setup

BM@N is a fixed target experiment at the NICA accelerator complex focused on the production of strange matter in heavy-ion collisions at beam energies between 2.0 and 6.0 AGeV. The primary setup consists of a large-acceptance dipole magnet with a magnetic field up to 1.2 T. Inside the magnet a target is placed and along with it there are inner tracking detector modules based on one plane of a forward silicon detector and 6 GEM (Gas Electron Multiplier) detector stations. The outer tracking module consist of Drift Chambers (DCH), Time-of-Flight detectors (TOF), Cathode Strip Chamber (CSC) and ZDC (Zero-Degree Calorimeter) to identify and measure the particles [2-4].

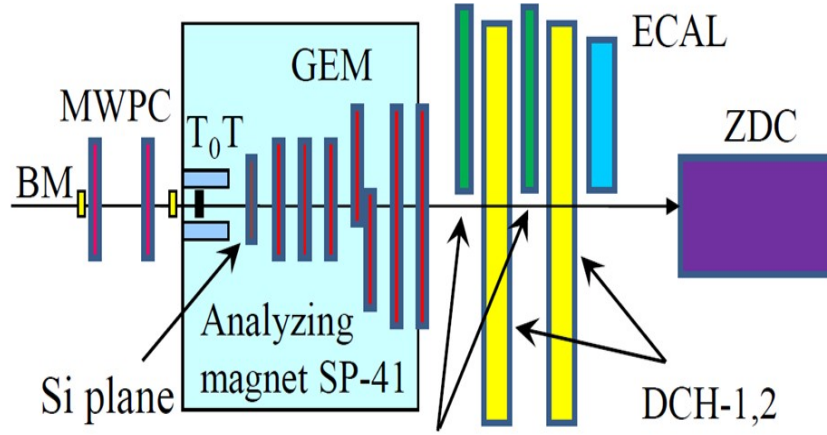


Fig. 3 - BM@N setup in the carbon beam run (RUN 6)

A GEM is a type of gaseous ionization detector which collects electrons released by ionizing radiation, guiding them to a region with a large electric field, and thereby initiating an electron avalanche. GEMs are a category of micropattern gaseous detectors. Under optimum conditions and in the presence of appropriate gases, a single electron entering any hole (made by acid etching process) will create an avalanche containing 100 –1000 electrons; this is the "gain" of the GEM. Since the electrons exit the rear of the GEM, a second GEM placed after the primary one will provide a further stage of amplification. More the amount of GEM stacks, more the gain (sometimes over a million).

For Run-6 of BM@N, the magnetic field at the center of the analyzing magnet was 0.61 T and the tracking stations were arranged so that the beam passed through their centers (Fig. 3). The 6 GEM stations were combined from 5 GEM detectors with the size of 66x41 cm<sup>2</sup> and 2 GEM detectors with the size of 163x45 cm<sup>2</sup>.

## 2 Track reconstruction of $\Lambda^0$ -hyperons

Reconstruction of charged particle trajectories is a crucial step in the event reconstruction procedure. An algorithm used to this aim needs to be quite flexible and swift. The analysis of reconstructed tracks - candidates of  $\Lambda^0$ -hyperons (*invariant mass* = 1.12 GeV/c<sup>2</sup>) at the GEM stations and track residuals corrections in Run-6 have been presented in this paper.

After certain modifications of the respective profiles of the track residuals, the corrections were incorporated into the BmnRoot software, individually for different targets: C, Al, Cu, Pb. These corrections are a significant part of the analysis. They compare and improve the accuracy of the track reconstruction procedure for Monte-Carlo and physical events ; and further enhances the measurement precision of the cross sections and yields of  $\Lambda^0$  in C+C, C+Al, C+Cu, C+Pb reactions for 4.5 GeV collision energy.

The method for reconstructing the track was based on the "cellular automation" approach, in which the cell is considered as a basic element of the algorithm. Here, "cell" refers to a line segment connecting two hits belonging to different levels of the inner tracker composed of GEM and silicon trackers [5]. The extrapolated and reconstructed points were obtained using Kalman filter smoothing functions.

$\Lambda^0$  hyperons were reconstructed using their decay mode into two oppositely-charged tracks. All positive tracks were assumed to be protons ( $p^+$ ) (*rest mass* =  $0.938 \text{ GeV}/c^2$ ) and all negative as negative pions ( $\pi^-$ ) (*rest mass* =  $0.14 \text{ GeV}/c^2$ ), because no particle identification was utilized in the analysis. The major selection criteria for  $\Lambda^0$  hyperons track candidates is that a track needs a minimum of 4 hits in the 6 GEM stations. For 4.5 AGeV carbon beam data, the momentum range for positive tracks was  $p_{\text{pos}} < 4.4 \text{ GeV}/c$  and for negative tracks  $p_{\text{neg}} > 0.3 \text{ GeV}/c$ .

## 2.1 GEM dx-residuals of reconstructed track

After applying selection criterias to the reconstructed tracks, two-dimensional profiles of the dx-residual distribution for positive and negative tracks for all GEM stations and for different targets were constructed (Figures 4 – 7). In terms of axis notations “dxsmo” is difference between the x-coordinate of the reconstructed track hit at z position of the GEM detector station and the x-coordinate of the extrapolated track hit, while “xsmo” is the extrapolated x-coordinate of track hit in GEM station.

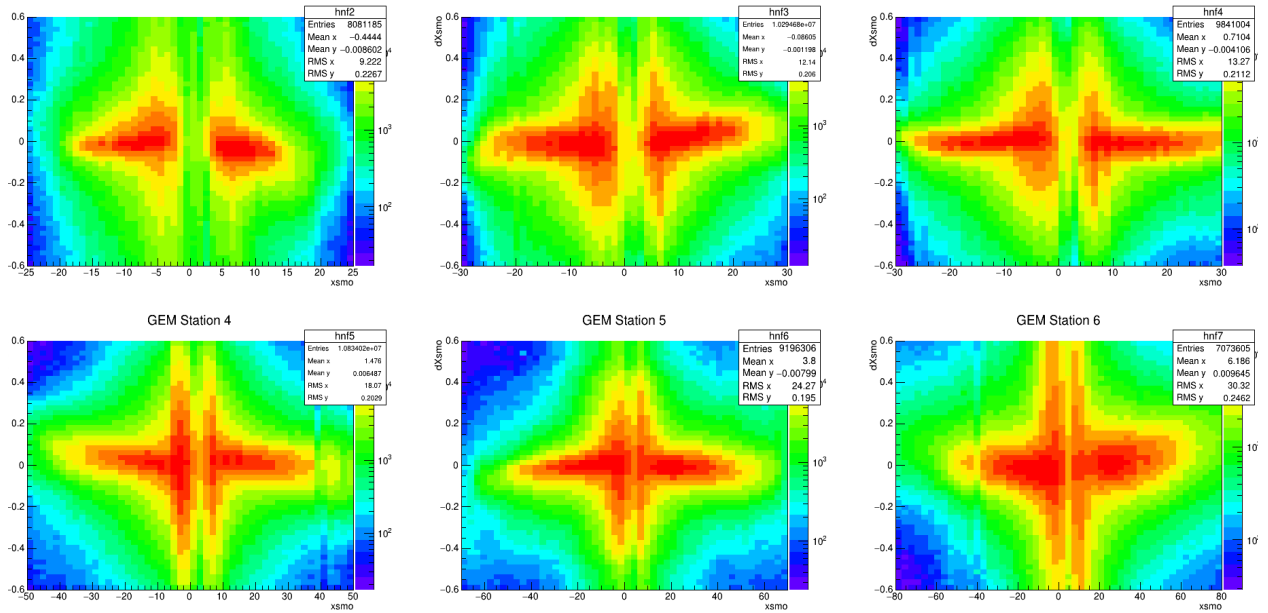


Fig. 4 - profiles of the dx-residual distribution for positive and negative tracks for all GEM stations for C + AI dataset

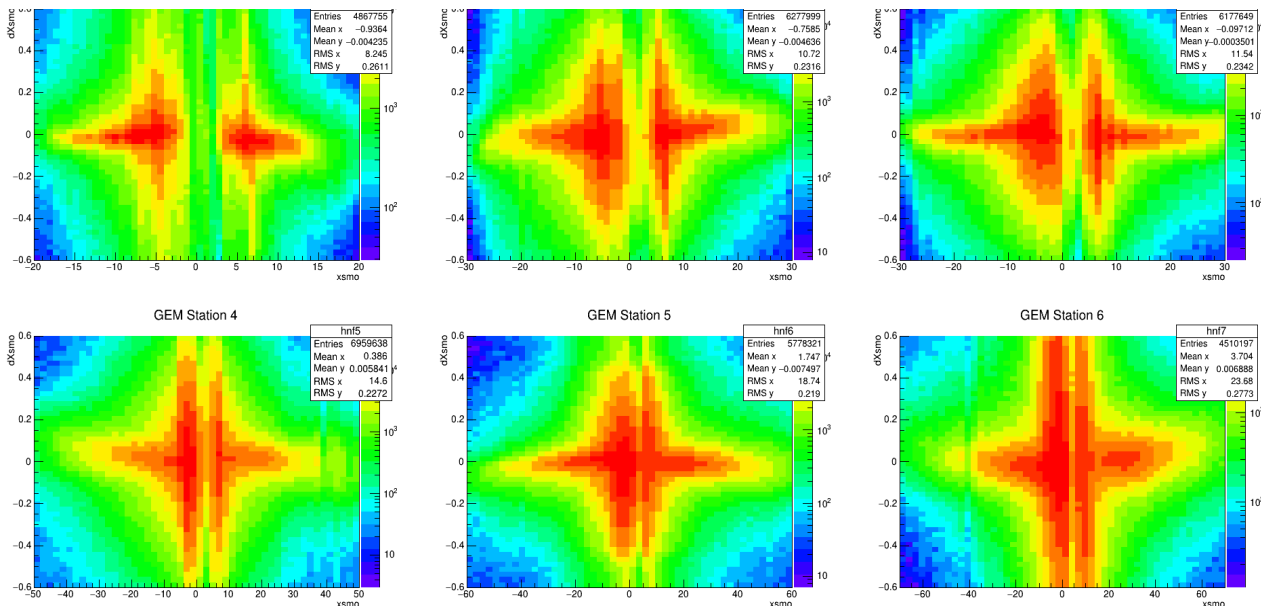


Fig. 5 - profiles of the dx-residual distribution for positive and negative tracks for all GEM stations for C + C dataset

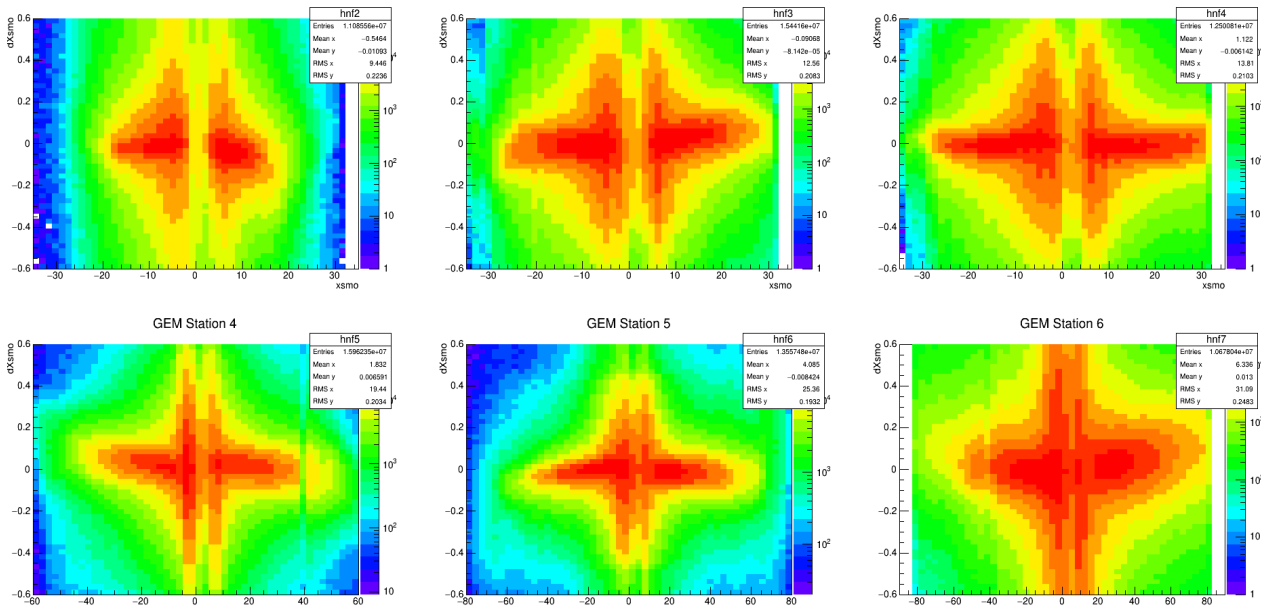


Fig. 6 - profiles of the  $dx$ -residual distribution for positive and negative tracks for all GEM stations for  $C + Cu$  dataset

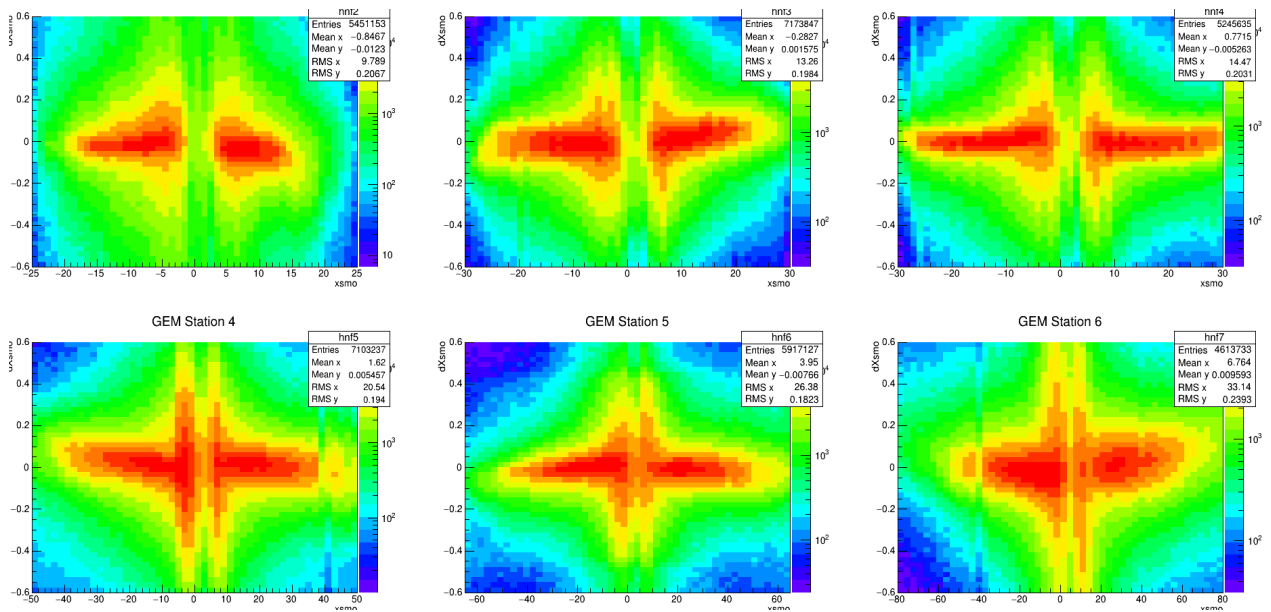


Fig. 7 - profiles of the  $dx$ -residual distribution for positive and negative tracks for all GEM stations for  $C + Pb$  dataset

### **2.1.1 dx-residuals corrections**

Distributions in Figures 4-7 illustrate that the position of the dx-residual values along  $x$  -axis is not at zero, so we must make their corrections. First, we sliced two-dimensional profiles of the dx-residual distribution along  $x$ -axis. After that the obtained dx-residuals slices for each station were fitted with a combination of Gaussian and second-degree polynomial functions.

Using extracted mean parameter and extracted error of the Gaussian part function, the 1-dimensional distributions were obtained. These profiles were fitted with 5 order-degree polynomial functions (Figure 8 for C+Cu process). These new fit functions were integrated to BmnRoot package code and new corrected dx-residuals were obtained. The final values for the dx-residuals were acquired and applied after a few correction iterations (Figure 9).

A before-and-after correction comparison of C+Cu is demonstrated in Figure 10. In Figures 11 -13, a similar comparison is shown for the other 3 targets. For a concrete comprehension of the analysis, a comparison of all targets before correction and that of after correction are presented in Figures 14 and 15 respectively.

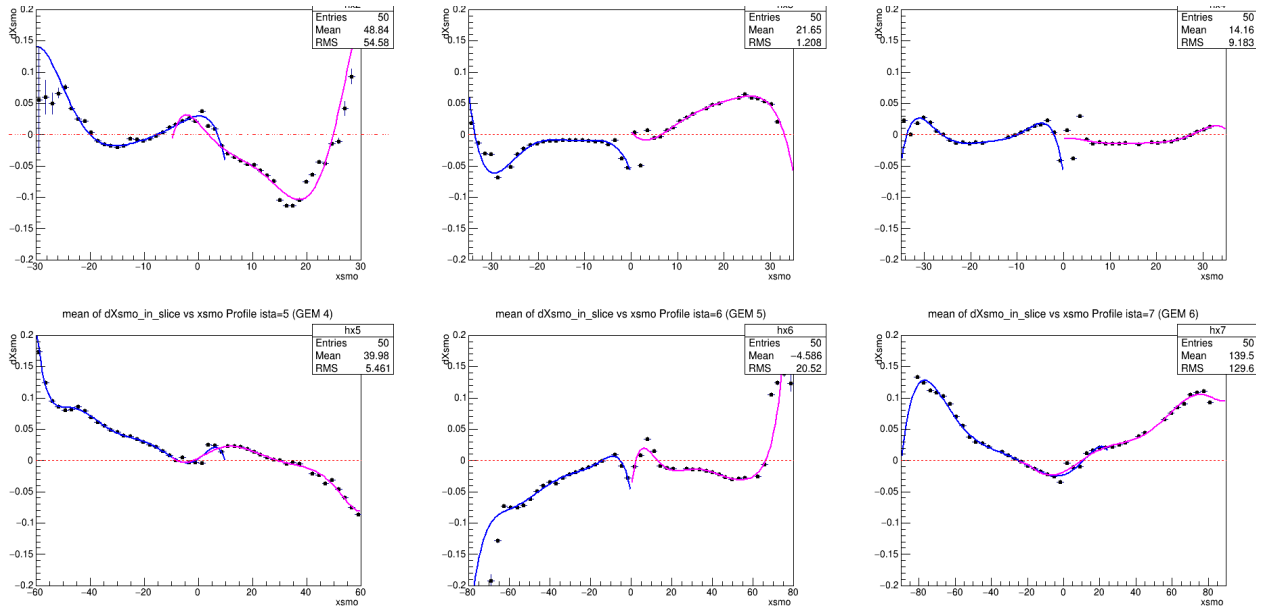


Fig. 8 - Mean  $dx$ -residuals vs.  $x$  for all GEM stations for  $C + Cu$  (Before Corrections)

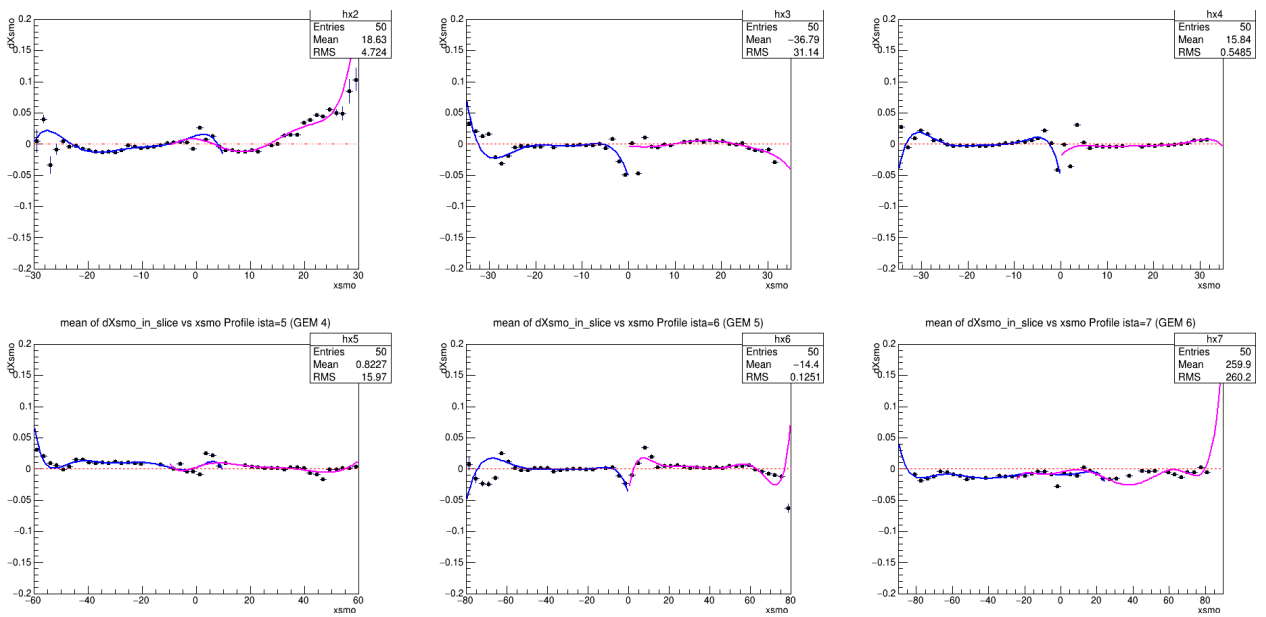


Fig. 9 - Mean  $dx$ -residuals vs.  $x$  for all GEM stations for  $C + Cu$  (After Corrections)

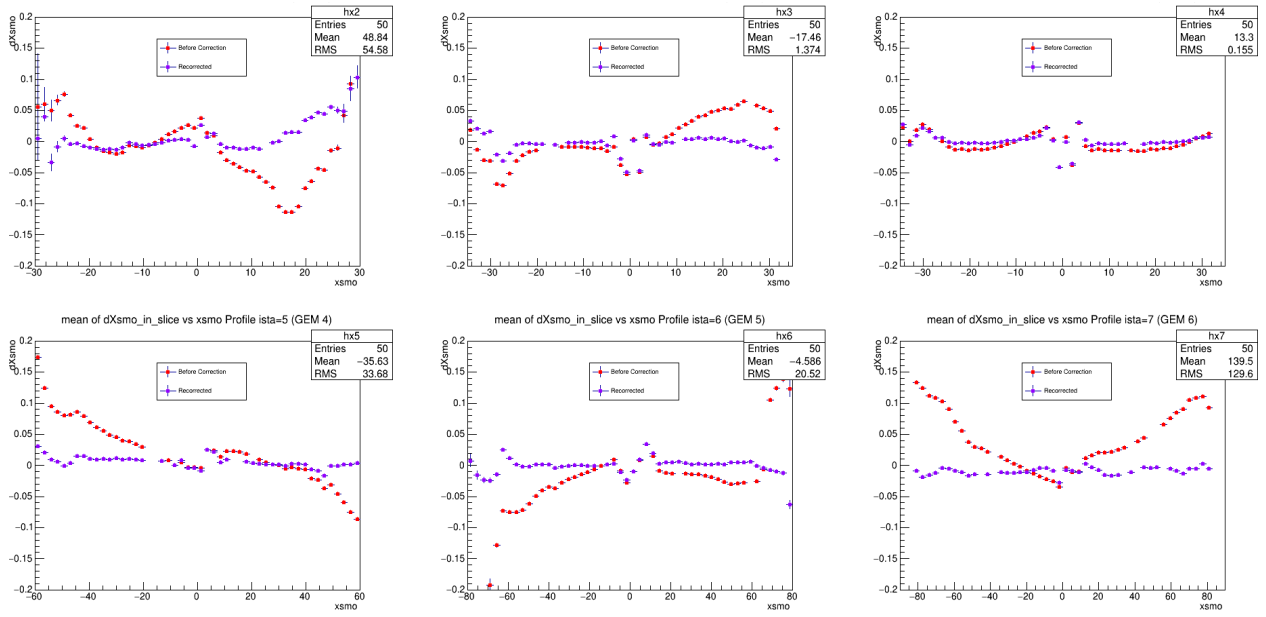


Fig. 10 - Mean  $dx$ -residuals vs.  $x$  for all GEM stations before-and-after correction comparison for the  $C+Cu$  process

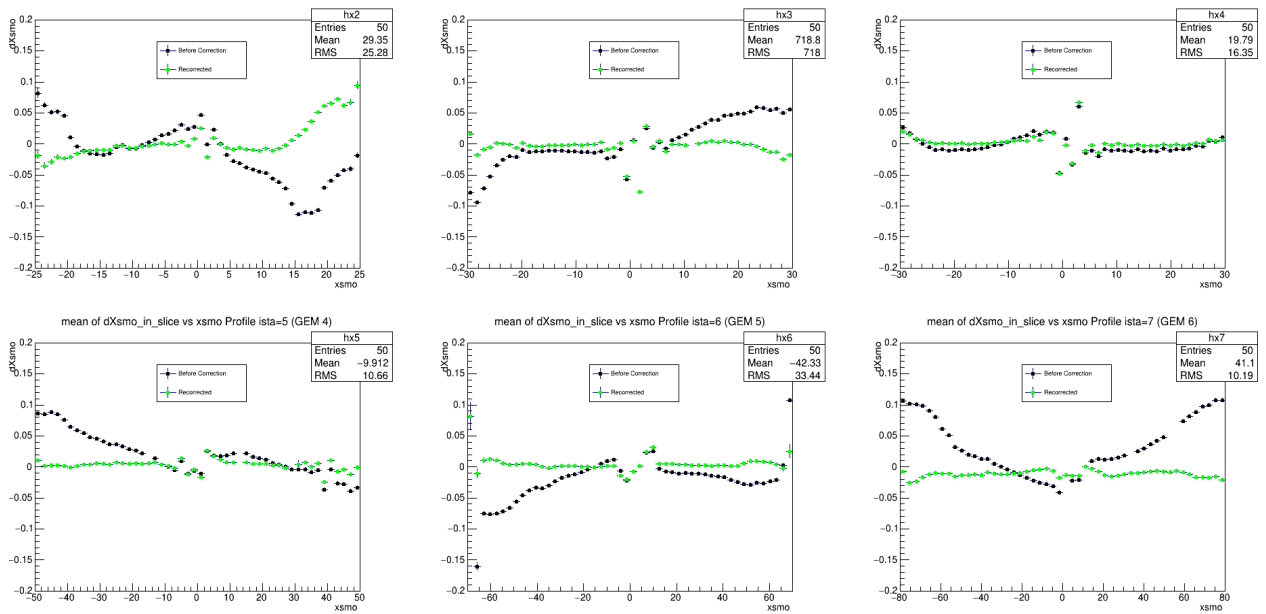


Fig. 11 - Mean  $dx$ -residuals vs.  $x$  for all GEM stations before-and-after correction comparison for the  $C+Al$  process

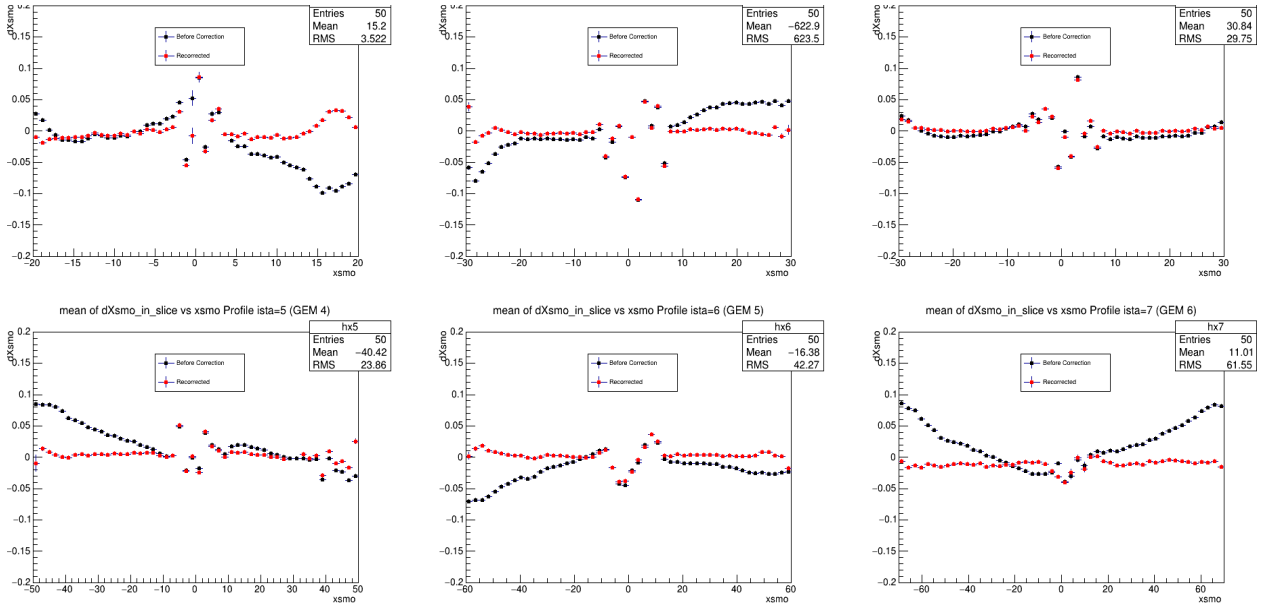


Fig. 12 - Mean  $dx$ -residuals vs.  $x$  for all GEM stations before-and-after correction comparison for the C+C process

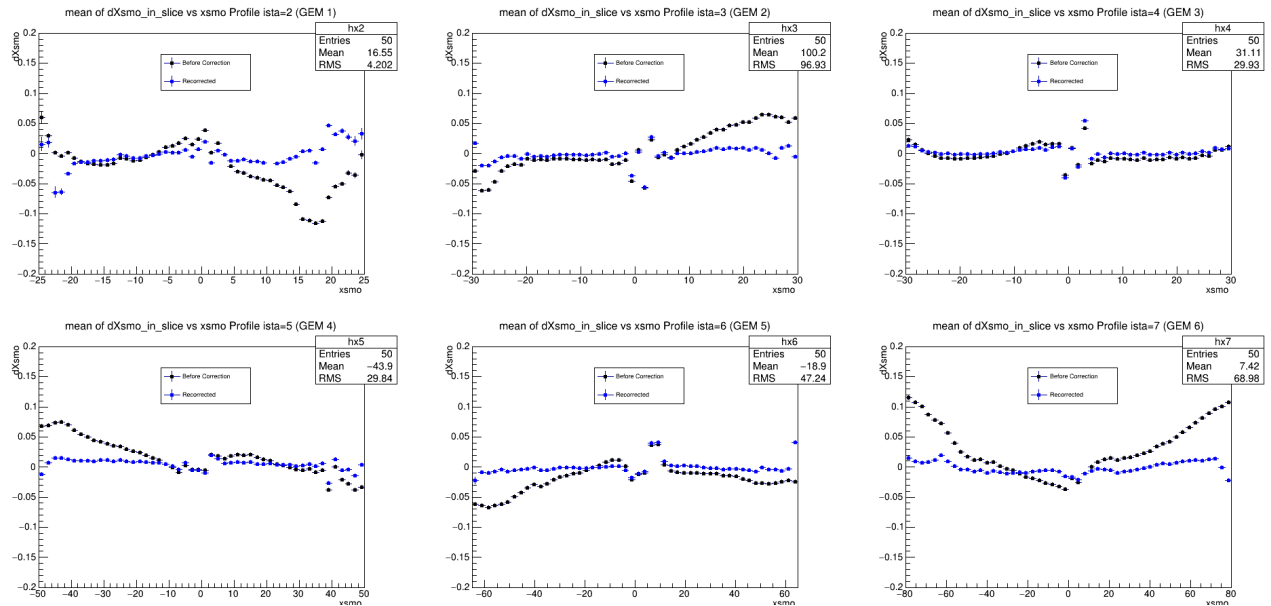


Fig. 13 - Mean  $dx$ -residuals vs.  $x$  for all GEM stations before-and-after correction comparison for the C+Pb process

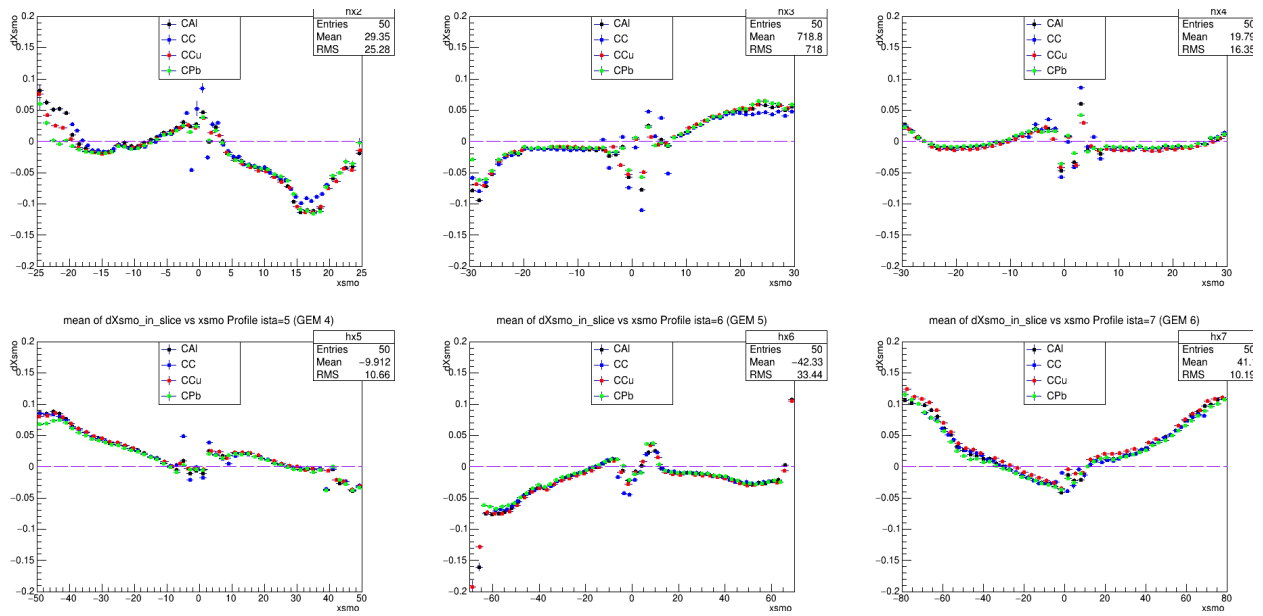


Fig. 14 – Mean  $dx$ -residuals vs.  $x$  for all GEM stations before  $dx$ -corrections for all targets

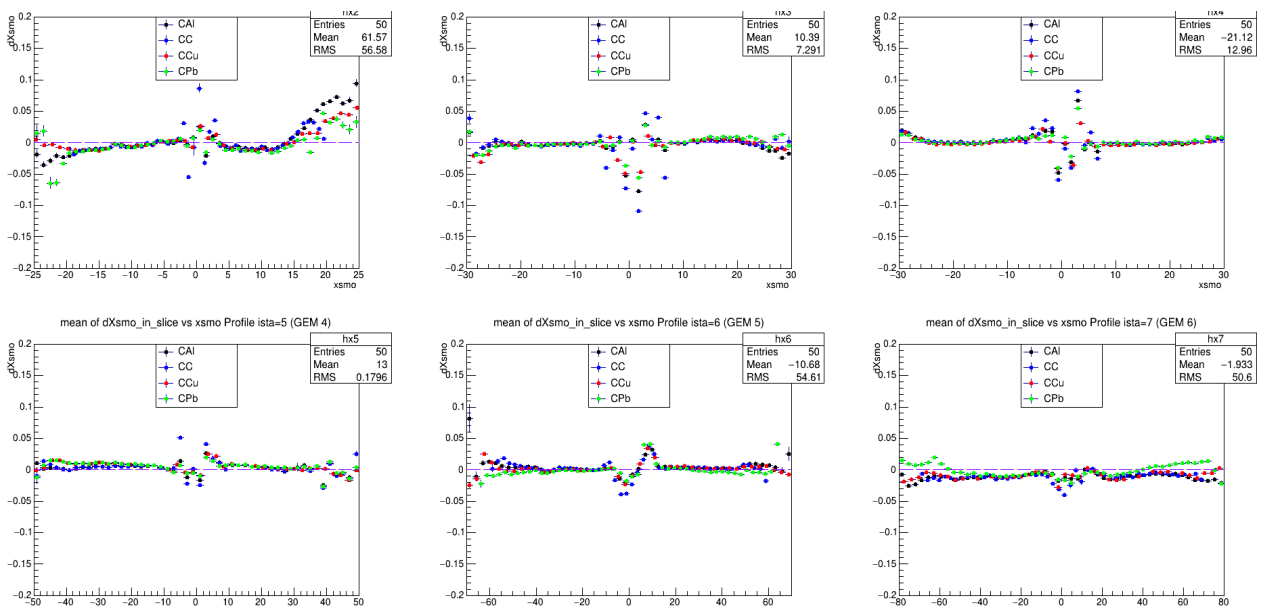


Fig. 15 – Mean  $dx$ -residuals vs.  $x$  for all GEM stations after  $dx$ -corrections for all targets

## 2.1.2 Errors of the dx-residuals determination

Extracted parameter sigma from the Gaussian part of fit and its error were used in the same way to construct 1-dimensional profiles to estimate the errors of dx-residuals determination. Figures 16 and 17 show, respectively, a comparison of the error distribution of the dx-residuals determination for all targets before and after corrections in terms of sigma.

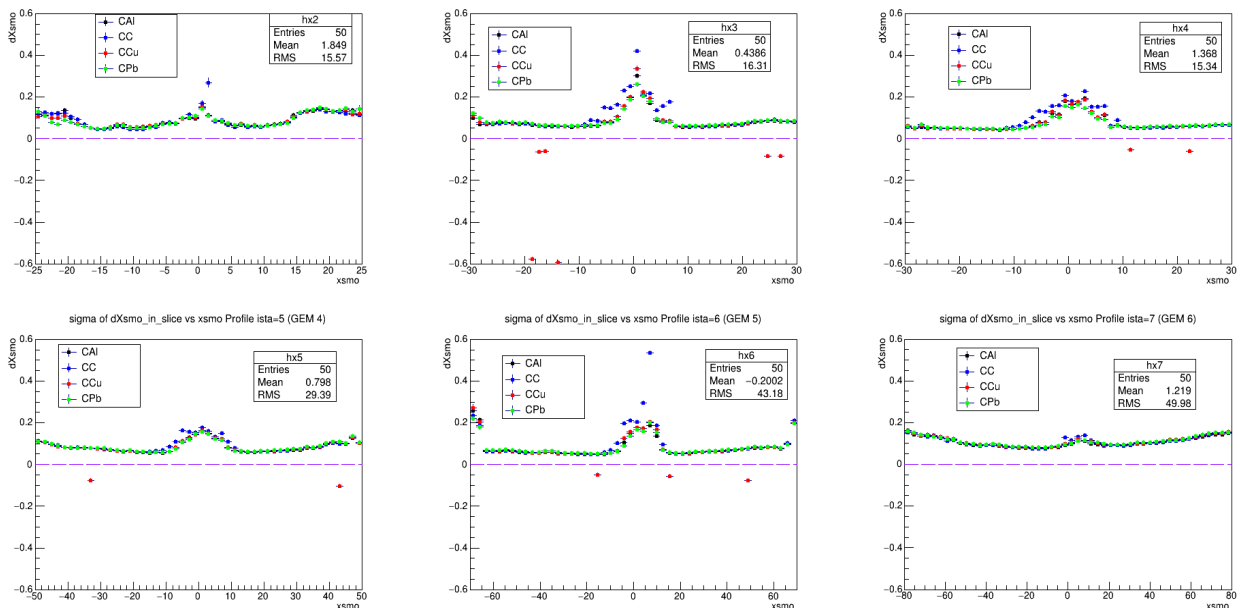


Fig. 16 - Errors of the dx-residuals determination vs.  $x$  for all GEM stations before corrections

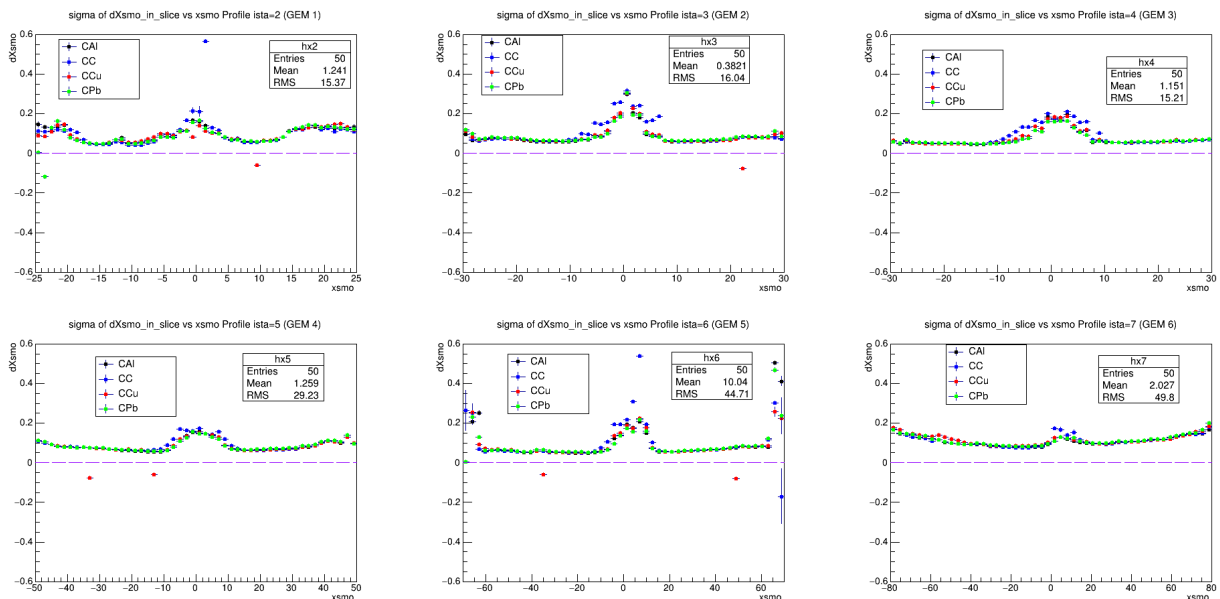


Fig. 17 - Errors of the dx-residuals determination vs.  $x$  for all GEM stations after corrections

### 3 Conclusion

The procedure of the dx-residual corrections has been successfully applied for physical dataset for Run-6 for all targets at beam energies of 4.5 GeV. The corrected distributions show that the corrections to the dx-residuals were calculated and applied correctly. For dx-residual errors, these are unchanged before and after correction. Therefore, the corrections do not affect the errors of dx-residual determination.

The results obtained are compared with the simulated events in Monte-Carlo. Monte-Carlo simulations should be included with these modifications to match the experimental data. And finally, at the end of the analysis, more accurate and precise values of the yield and cross section of the  $\Lambda^0$  hyperon are obtained.

### References

- [1] K. Alishina et al., *Physics of Particles and Nuclei Letters*, Vol. 19, No. 5, pp. 485–488 (2022)
- [2] P. Batyuk et al., *EPJ Web of Conferences* 214, 05027 (2019)
- [3] J. Adams et al., *Nucl. Phys. A* 757, 102-183 (2005)
- [4] K. Adcox et al., *Nucl. Phys. A* 757, 184-283 (2005)
- [5] D. Baranov et al., *EPJ Web of Conferences* 226, 03003 (2020)

### Acknowledgement

I want to express my gratitude to the START Team for providing students with such a tremendous opportunity to engage in ongoing research in the field of nuclear science. I appreciate the support and encouragement I received from my supervisor, Mr. Yury Stepanenko, who helped me comprehend the BM@N experiment software's interface as well as the technique and methodology of the modifications necessary to get enhanced reconstructed distributions. I'm quite happy that this internship allowed me to get knowledge of the specifics of high energy physics experimental data processing.